Study of Structural, Morphological and Optical Properties of Spray Deposited Sn Doped B - V_2O_5 Thin Films

T Akkila[a]* , I Mansur Basha[a, b]
[a]PG & Research ,Department of Physics, Govt. Arts College, Trichy,Tamilnadu, India
[b]PG & Research, Department of Physics, Jamal Mohamed College (Autonomous), Trichy, Tamilnadu, India

ABSTRACT

Vanadium pentoxide (V_2O_5) thin films doped with Sn (insteps of 0.1mM of Sn) were deposited onto glass substrates using spray pyrolysis technique. The structural, morphological, and optical properties of the films were investigated. XRD patterns of as - deposited films confirmed the polycrystalline nature of the films with orthorhombic structure and annealed films confirmed the formation of β - V_2O_5 phase. Crystallite size increased with an increase of annealing temperature. Scanning Electron Micrograph of annealed film shows the formation of overlapped rods like morphology. The band gap was obtained from Tauc's plot and found to vary from 2.32 to 2.52eV for as - deposited films and 2.22 to 2.28 eV for annealed films. The effect of annealing temperature was analysed and discussed.
Keywords: Thin Films; Spray Pyrolysis; B - V_2O_5; X - Ray Diffraction

I. INTRODUCTION

In recent years, the formation of nanostructures with the properties of the metal - oxide thin films mainly depends on the synthesis method. Over such competing methods, spray pyrolysis plays a vital role in the synthesis of quality films with different nanostructured metal oxide thin films. It is a modest and inexpensive method used for large area depositions with good uniformity and porosity in films [1] and yields oxide films of high quality at rather low costs when properly controlled. Spray pyrolysis offers a list of controlling parameters such as solution molarity, substrate temperature, annealing temperature, annealing time, and dopant effects. In spray pyrolysis method particle formation is mainly depended on the shape of the droplet sprayed on preheated substrate, so it avoids the formation of clusters initially. The size of the droplets can be monitored at nanoscale at low temperature [2]. Spray pyrolysis is not limited to specific metal oxide and it is widely used to prepare various metal oxides.

Among different metal oxides, synthesis of V_2O_5 thin films at low temperature has become a challenging one. V_2O_5 is known for its multivalency, layered structure, wide optical band gap, good chemical and thermal stability, excellent thermoelectric property [3]. On the other hand, interest was developed in the preparation of doped V_2O_5 thin films. The advantage of doping different metal ions into V-O lattice enables one to alter the microstructure, morphology, electrical and optical properties. Besides these, the central platform of doped V_2O_5 thin films has emerged in enhancing the electrochemical performance and Lithium ion insertion. Researchers have synthesized doped V_2O_5 thin films with different metals such as Ag [4], Mo [5], Sn [6], Zr [7], Na [8], F [9], Cu [10], and Cr [11] by using various methods. Regarding Sn, itis considered as most promising dopant since its valence state (Sn^{4+}) is near to the valence state of V_2O_5 (V^{5+}) and the ionic radius of Sn^{4+} (0.69Å) is just greater than V^{5+} (0.59Å). By such way of doping a low valence cation into V_2O_5 lattice can modify the growth kinetics considerably.

In this connection, we aim to prepare Sn - doped V_2O_5 thin films by spray pyrolysis method and mainly focused on the structural, morphological and optical properties of V_2O_5 thin films by doping the Sn content and also investigated the annealing effect on the Sn - doped V_2O_5 thin films. In the present work, we studied the doping and annealing effect of Sn in V_2O_5 at different concentrations of Sn and structural, morphological, and optical properties of prepared samples are reported.

II. MATERIALS AND METHODS

A. Film deposition

Pristine and Sn - doped vanadium pentoxide thin films have been deposited onto glass substrate by spray pyrolysis system. A home built spray system was constructed as reported by Jeyaprakash et al [12]. The glass substrates were cleaned chemically and dried to remove the unwanted organic matters present in the substrate. The cleaned glass substrates were placed on the heater which is controlled by chrome-nickel thermocouple fed to a temperature controller with an accuracy of ±1˚C. For pristine V_2O_5 thin film 0.05M of vanadium (III) chloride [VCl_3] was dissolved in 50 ml of deionized water. For Sn-doped V_2O_5 thin films a suitable amount of tin (IV) chloride ($SnCl_4.5H_2O$) was added from 0.01mM to 0.05mM insteps of 0.01mM in the precursor solution respectively. The solution was sprayed at an angle of 45˚ onto preheated glass substrate kept at a distance of 50cm from the spray gun. Compressed dry air at a pressure of 2 kg/cm^2 from an air compressor via an air filter - cum regulator was used as the carrier gas and spray rate of the solution was maintained at 3 ml/min. To avoid excessive cooling of substrates, successive spraying process was used with time period of 15 seconds between two sprays. All the prepared film samples were annealed at 300°C for 1 hour in air atmosphere.

B. Characterization techniques

The structural details of the prepared thin films were carried out by P Analytical X-ray diffractometer (Model D/MAX ULTIMA III) using Ni- filtered CuKα X-radiation (λ=1.54056Å). A range of 2θ from 10° to 100° was scanned from a fixed slit type, so that all possible diffraction peaks could be detected. Crystallite size and micro strain were analyzed by X-Ray line broadening technique. Surface morphology of the films was investigated by using Field Emission Scanning Electron Microscope (Model Carl Zeiss ultra 55) with an accelerating potential of 18KV. Prior to imaging, the films were sputtered with a thin gold film to enhance the emission of the secondary electron for better imaging. The optical properties and band gap of the thin films were analyzed by UV-VIS-NIR spectrophotometer (Model- Lambda 35).

III. RESULTS AND DISCUSSION

A. Structural analysis

Figure 1 shows XRD pattern of pure and Sn-doped V_2O_5 as - deposited thin films. The pureV_2O_5 thin film has a polycrystalline nature with the preferred orientation along (0 0 1), which indicates α - V_2O_5 at 2θ ≈ 20.1 with orthorhombic structure (JCPDS #41 - 1426) and additional peaks along (1 0 1), (1 1 0) and (1 0 0) are observed. The plane (2 0 0) corresponds to β - V_2O_5 phase with the tetragonal structure (JCPDS #45- 1074).

As the dopant concentration increased from 0.01 mM to 0.03mM, (0 0 1) plane has disappeared and the orientation along (1 1 0) plane evolved. Intensity levels of doped V_2O_5 have decreased with an increase of dopant concentration from 0.01mM to 0.03mM and may be attributed due to the less crystallite size. Films prepared at 0.04mM and 0.05 mM showed amorphous natures.
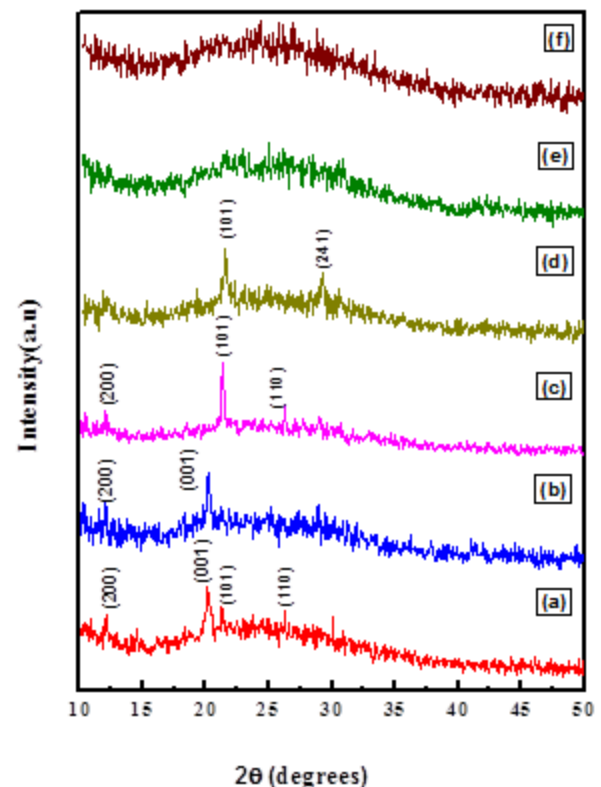
Figure 1. XRD patterns of as - deposited (a) pure V_2O_5 and
Sn - doped (b) 0.01 mM (c) 0.02 mM (d) 0.03 mM (e) 0.04 mM (f) 0.05 mM

Figure 2 depicts XRD pattern of pure and Sn-doped V_2O_5 annealed thin films. All the annealed films exhibit a good degree of crystallinity. The pristine and Sn - doped V_2O_5 thin films at 0.01 and 0.02mM concentrations showed a single sharp peak with polycrystalline nature. Interestingly there is no evidence for α - V_2O_5 phase, only β - V_2O_5 phase has appeared with sharp peak along (2 0 0) plane at 2θ ≈ 12.6. Intensity trend for these planes increases as dopant concentration increases from 0.03 to 0.05mM meanwhile the intensity of (2 0 0) plane has decreased.
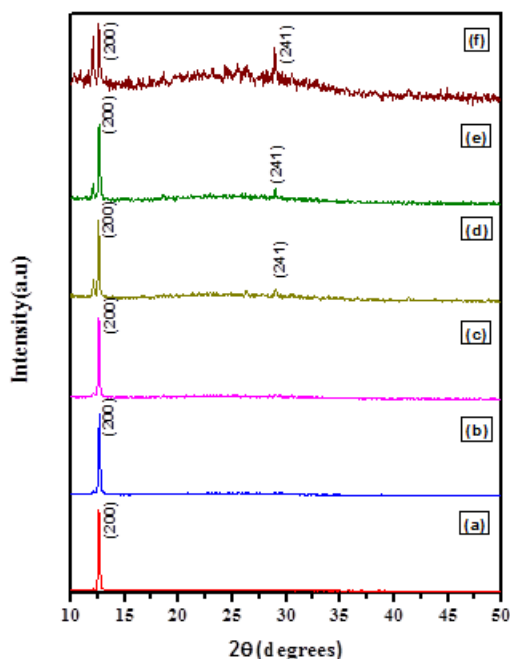
Figure 2. XRD pattern of annealed (a) pure V_2O_5 and Sn - doped (b) 0.01 mM (c) 0.02 mM (d) 0.03 mM (e) 0.04 mM (f) 0.05 mM

Earlier reports [13 - 16] confirmed the formation of β - V_2O_5 phase at various preparing conditions by using various methods. In our work, the phase transformation is achieved by an annealing process at low temperature (300°C) by using spray pyrolysis method. Furthermore, the significance of Sn doping is evident from the XRD patterns. An inclusion of Sn in the V - O lattice couldn't yield much change and failed to accommodate into the VO_5 layers. But after annealing, Sn^{4+} ions gain enough mobility to accommodate into VO_5 slabs and results in destruction of β - V_2O_5phase. The accommodation of Sn^{4+} ions into VO_5 layers with decrease in intensity of diffraction peak by annealing treatment was reported by Y. Li et al [6] at 450°C. As the dopant concentration increased from 0.01mM to 0.05mM, the crystallinity of the films has been restored partially and could able to alter the structural properties of V_2O_5.

The crystallite size and microstrain were calculated by using Scherrer's formula [17],

$$D = 0.9\lambda / \beta\cos\theta \text{ and } \varepsilon_{hkl} = \beta/4\tan\theta$$

where, D is size of the grain in the direction perpendicular to the reflecting planes, θ is diffraction angle, K is shape factor (=0.9), λ is wavelength of X-ray, β is the full width at half maximum of prominent peaks in radian and ε_{hkl} is microstrain. Crystallite size of annealed thin films increased than that of as - deposited one, which was attributed to variation in thickness of the thin films. Table 1 gives the information about the crystallite size, microstrain, and FWHM values of as - deposited and annealed thin films at various concentrations.

B. Morphological studies

Figure 3 and 4 illustrate the surface morphologies of as - deposited and annealed pristine V_2O_5 and Sn - doped V_2O_5 thin films. There is a noteworthy difference between before and after annealing. Initially, the as - deposited pristine V_2O_5thin film (Figure 3a) exhibits a glassy surface with small grains. As the Sn dopant concentration increased, the morphology seems to be distorted (Figure 3d).It reflects the poor crystalinity and confirmed by the XRD results.

The annealed pure V_2O_5 thin film consist of intermeshed nano particles stacked over each other and look rod - like morphology which is due to the formation of new phase (β - V_2O_5). Fig (4b) - Fig (4d) indicates that the insertion of Sn^{4+} ions inhibits the formation of such intermeshed rods observed in pure V_2O_5 thin film. A similar effect was reported in the V_2O_5 thin films prepared by sol - gel method followed by annealing at 450°C [6]. As observed in fig 3d, the intermeshed rods have disappeared and particles exhibit flower petal like morphology. It could be caused by distortion of β - V_2O_5 phase at 0.05mM concentration of Sn. Figure 5 shows the SEM cross sectional images of prepared samples.

C. Optical studies

Figure 6 and 7 show the optical absorption spectra of as - deposited and annealed pristine V_2O_5 and Sn - doped V_2O_5 thin films. The as - deposited and annealed pristine V_2O_5 thin films have higher absorption values when compared with the doped ones. The absorption decreases when the concentration of Sn increases from 0.01 to

Table 1. Crystallite size, microstrain, and FWHM values of as - deposited and annealed thin films at various concentrations

| Sn dopant concentration	2θ (degrees)		FWHM (radian)		crystallite size (D) (nm)		Microstrain (ε_{hkl})	
	As deposited	annealed	As deposited	annealed	As deposited	annealed	As deposited	annealed
0	20.15	12.60	0.017453	0.002879	8.06	48.16	0.005639	0.006513
0.1	20.18	12.63	0.004014	0.002757	55.08	50.30	0.02455	0.006231
0.2	21.34	12.586	0.003141	0.002338	44.91	59.28	0.004168	0.005301
0.3	21.30	12.558	0.004886	0.002251	28.36	61.58	0.006496	0.005115
0.4	----	12.615	----	0.002879	----	48.16	----	0.006513
0.5	----	12.60	----	0.002443	----	57.10	----	0.005532
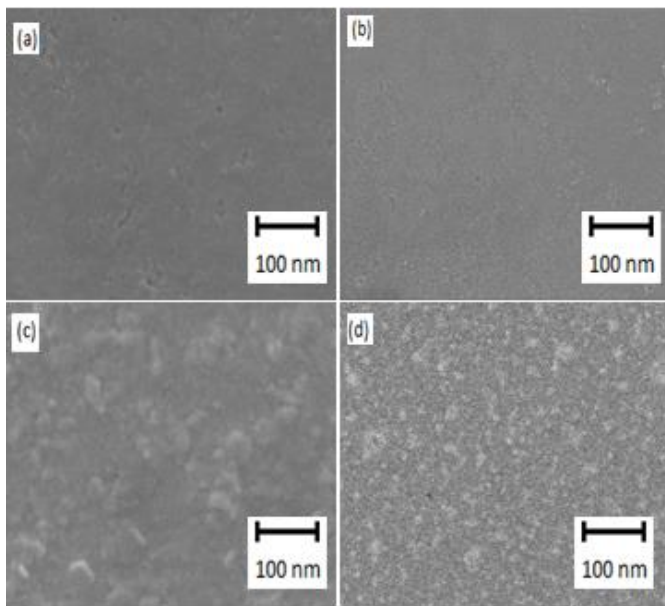
Figure 3. FESEM images of as - deposited (a) pure V_2O_5 and
Sn - doped (b) 0.01 mM (c) 0.03 mM (d) 0.05 mM

0.03 mM. The trend is reversed in case of 0.04 and 0.05 mM concentrations. of Sn, which could resulted from amorphous nature of the films. After annealing, the absorption of Sn - doped V_2O_5 samples is enhanced due
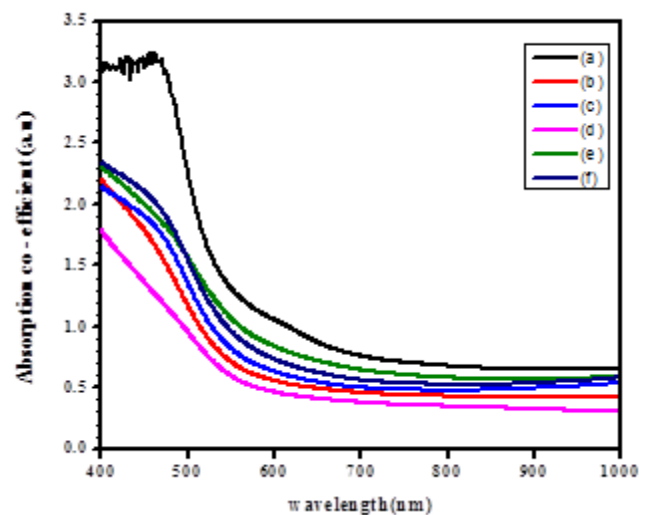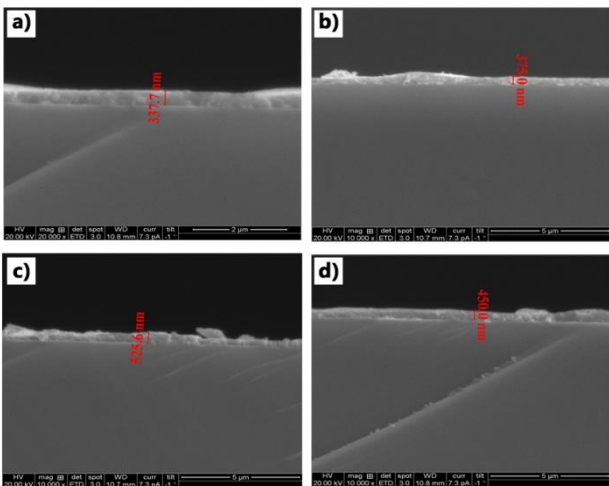

Figure 6. UV - VIS absorbance spectrum of as - deposited (a) pristine V_2O_5 and Sn doped (b) 0.01 mM (c) 0.02 mM (d) 0.03 mM (e) 0.04 mM (f) 0.05 mM

Figure 8 and 9 depict the optical transmittance spectra of the as-deposited and annealed pristine and Sn - dopedV_2O_5 thin films observed in the wavelength range of 400 - 1000 nm. As seen from the graph that the transmittance of Sn - doped V_2O_5 higher than pristine V_2O_5. In the case of annealed films, a sharp absorption edge was observed at 500nm.
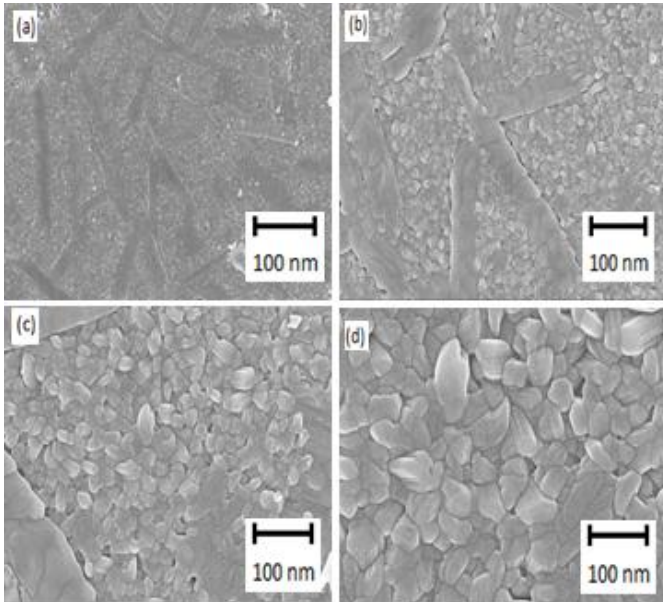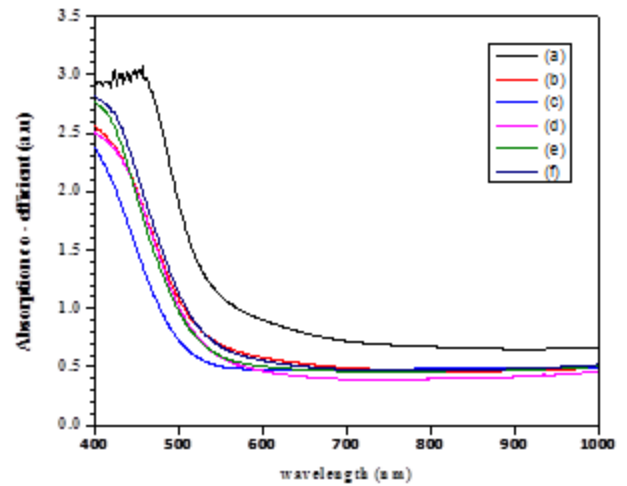
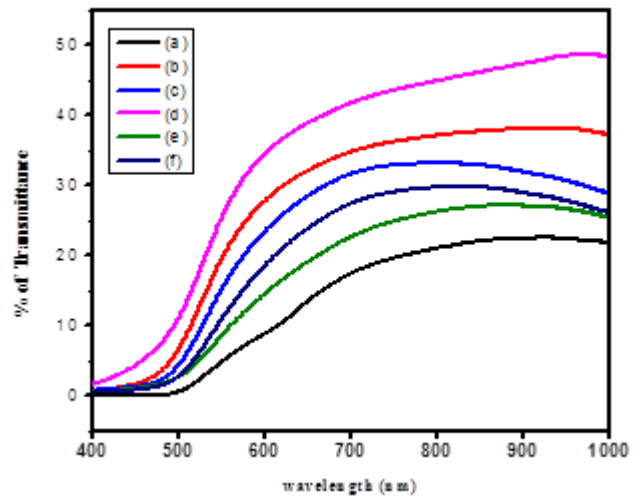**Figure 4.** FESEM images of annealed (a) pure V_2O_5 and Sn - doped(b) 0.01 mM (c) 0.03 mM (d) 0.05 mM

Figure 5. SEM Cross sectional images of as - deposited (a) pure V_2O_5 and Sn - doped (b) 0.04 mM (c) 0.05 mM(d) annealed Sn - doped 0.03 mM.

Figure 10 and 11 shows a plot of $(\alpha h\nu)^2$ vs hν to determine direct allowed band gap energy of as - deposited and annealed pure V_2O_5 and Sn - doped V_2O_5 thin films. The optical band gap energies of as - deposited pure V_2O_5 is 2.32 eV. This value is consistent with the band gap energy of pure V_2O_5 (2.3eV) reported by S.F. Cogan et al [18].

Figure 7. UV - VIS absorbance spectrum of annealed (a) pure V_2O_5 and Sn - doped (b) 0.01 mM (c) 0.02 mM (d) 0.03 mM (e) 0.04 mM (f) 0.05 mM


Figure 8. UV-VIS transmittance spectrum of as - deposited (a) pure V2O5 and Sn - doped (b) 0.01 mM (c) 0.02mM(d) 0.03 mM (e) 0.04 mM (f) 0.05 mM
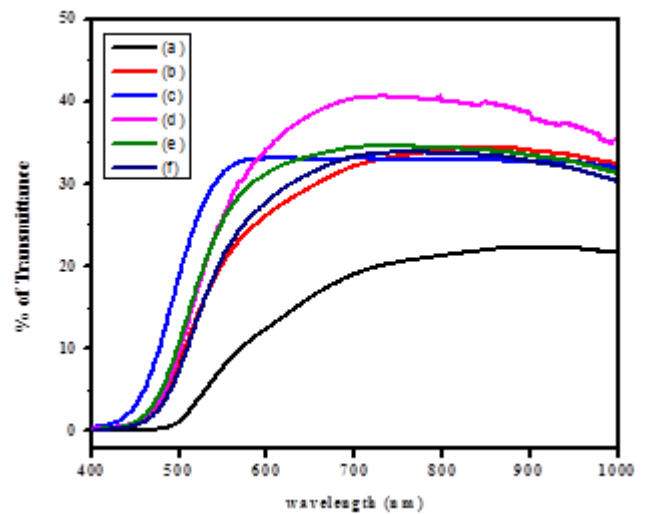

Figure 9. UV - VIS transmittance spectrum of annealed (a) pure

V2O5 and Sn - doped (b) 0.01 mM (c) 0.02 mM (d) 0.03 mM (e) 0.04 mM (f) 0.05 mM

Band gap energies of Sn - doped V_2O_5 thin films at different concentrations (0.01 to 0.05mM) are varied from 2.46 to 2.52eV. Accordingly, the observed slight increase of the optical band gap can be related to the distortion aided by the Sn^{4+}ions in the structure of V_2O_5 thin films which was confirmed by XRD and morphology of as - deposited films. The improved band gap energy can also be attributed to increasing in the transmittance as well as insulating nature of the prepared samples.
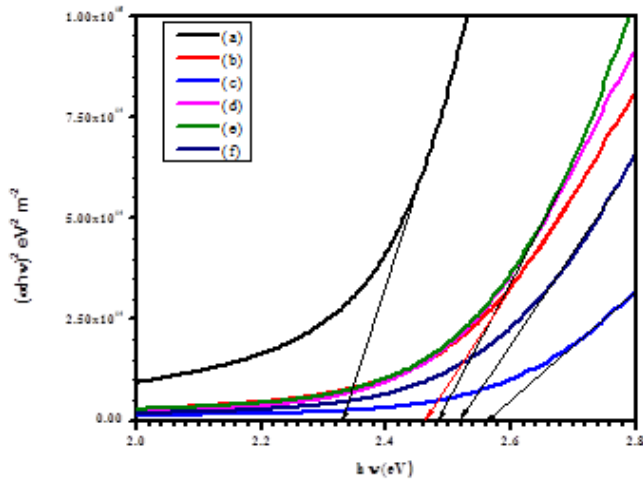
Figure 10. Plot of hνVs $(\alpha h\nu)^2$ of as - deposited (a) un doped V_2O_5 and Sn - doped (b) 0.01 mM (c) 0.02 mM (d) 0.03 mM (e) 0.04 mM (f) 0.05 mM
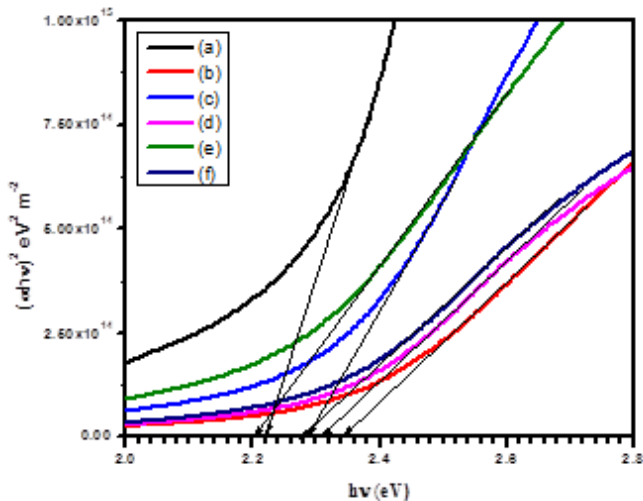
Figure 11. Plot of hνVs $(\alpha h\nu)^2$ of annealed (a) un doped V_2O_5 and Sn - doped (b) 0.01 mM (c) 0.02 mM (d) 0.03 mM (e) 0.04 mM (f) 0.05 mM

In case of annealed films the optical band gap energies of pure V_2O_5 is 2.22 eV, whereas for Sn- doped V_2O_5 films vary from 2.34 to 2.28 eV at different concentrations (0.01 to 0.05mM). Consequently, the decrease of the optical band gap at post-annealing temperature (300°C) can be associated to the new phase of V_2O_5 (β - V_2O_5) and increase in grain size of annealed films. The observed variation in the band gap energy of both as - deposited and annealed films may also be related to the degree of non-stoichiometry in the V_2O_5 [19].

IV. CONCLUSION

The pristine and Sn- doped V_2O_5 thin films were successfully prepared by spray pyrolysis method. The prepared samples were annealed at 300°C for an hour in air. The X-ray diffraction studies showed that the pristine V_2O_5 is in α - V_2O_5, whereas the dopant Sn altered the microstructure and lead to amorphous nature at higher concentration of Sn. After annealing, the pure V_2O_5 changed into β-phase. Formation of β - V_2O_5 phase from α - V_2O_5 phase at low annealing temperature (300°C) is interesting part of our work. Moreover, Sn^{4+} ions played its role in altering the microstructure in as - deposited and annealed films. SEM images showed that the inclusion of Sn^{4+} ions destructed the microstructure for as - deposited samples and inhibited the formation of intermeshed rods of pure V_2O_5 for annealed samples. The optical band gap energy of as - deposited and annealed pure V_2O_5 are 2.32 and 2.22 eV. The increase in band gap energy is observed for both as - deposited and annealed by doping Sn at different concentrations. The accommodation of Sn^{4+} within the layers of V_2O_5 may be an excellent candidate for gas sensing applications.

V. REFERENCES

[1]. A. Bouzidi, N. Benramdane, A. Nakrela, C. Mathieu, B. Khelifa, R. Desfeux, A. Da Costa, Mater Sci. Eng, B95 141-147 (2002)

[2]. D.S. Jung, Y.N. Ko, Y.C. Kang, S.B. Park, Adv. Powder Technol.25 18-31 (2014)

[3]. P. Chatterjee, S. P. Sen Gupta, S. Suchitra, Bull. Mater. Sci.24 173 (2001)

[4]. H.S. Hwang, S.H. Oh, H.S. Kim, W.I. Cho, B.W. Cho, D.Y. Lee, Electrochim. Acta 50 485-489 (2004)

[5]. A. Jin, W.Chen, Q. Zhu, Y. Yang, V.L. Volkov, G.S. Zakharova, Thin Solid Films 517 2023-2028 (2009)

[6]. Y. Li, J. Yao, E. Uchaker, M. Zhang, J. Tian, X. Liu, G. Cao, J. Phys. Chem. C,117 23507−23514 (2013)

[7]. H. Zhang, Z. Wu, X. Wu, X. Wei, Y. Jiang, Thin Solid Films56863-69 (2014)

[8]. M. M. E. Desoky, M. S. A. Assiri, A. A. Bahgat, J. Phys. Chem. Solids 75 992-997 (2014)

[9]. M. Abyazisani, M. M. Bagheri-Mohagheghi, M. R. Benam, Mat. Sci. Semicon. Proc.31 693-699 (2015)

[10]. H. Yu, X. Rui, H. Tan, J. Chen, X. Huang, C. Xu, W. Liu, D.Y. W. Yu, H.H. Hng, H.E. Hoster, Q. Yan, Nanoscale, 5 4937−4943 (2013)

[11]. S.Y. Zhan, C.Z. Wang, K. Nikolowski, H. Ehrenberg, G. Chen, Y.J Wei, Solid State Ionics,180 1198−1203 (2009)

[12]. B.G. Jeyaprakash, K. Kesavan, R. Ashok kumar, S. Mohan, A. Amalarani, Bull. Mater. Sci.34 601-605 (2011)

[13]. D. Vernardou, M. Apostolopoulou, D. Louloudakis, N. Katsarakis, E. Koudoumas, J. Colloid Interf. Sci. 424 1- 6 (2014)

[14]. K. Jeyalakshmi, S. Vijayakumar, K.K. Purushothaman, G. Muralidharan, Mater. Res. Bull. 482578-2582 (2013)

[15]. R. Santos, J. Loureiro, A. Nogueira, E. Elangovan, J.V. Pinto, J.P Veiga, T. Busani, E. Fortunato, R. Martins, I. Ferreira, Appl. Surf. Sci. 282590- 594 (2013)

[16]. D. Vasanth Raj, N. Ponpandian, D. Mangalaraj, C. Viswanathan, Mat. Sci.in Semicon. Proc.16 256-262 (2013)

[17]. A. Patterson, L. Phy. Rev.56 978 (1939)

[18]. S.F. Cogan, N.M. Nguyen, S.J. Perrotti, R.D. Rauh, J. Appl. Physics 66 1333-1337 (1989)

[19]. A.Z. Moshfegh, A. Ignatiev, Thin Solid Films198 251-268 (1991)